

Itinerant Ferromagnetism and Quantum Criticality in Sc_3In

A. Aguayo¹ and D.J. Singh

Center for Computational Materials Science, Naval Research Laboratory, Washington, DC 20375

¹ *also at School of Computational Sciences, George Mason University, Fairfax, VA 22030*

(November 12, 2018)

Abstract

The electronic structure and magnetic properties of hexagonal Sc_3In are calculated within density functional theory. We find that the Fermi energy lies in a region of flat Sc d derived bands leading to a peak in the density of states and Stoner ferromagnetism. The calculated local spin density and generalized gradient approximation spin magnetizations are both enhanced with respect to experiment, which is an indication of significant quantum critical fluctuations, neglected in these approximations. We find, as expected, that the ferromagnetism is initially enhanced under pressure, meaning that the critical point cannot be reached with modest pressure. However, we find that the density of states peak around the Fermi energy and the calculated density functional magnetic properties are sensitive to the c/a ratio, so that the quantum critical point may be reached under uniaxial strain.

A number of recent discoveries has lead to resurgence of interest in the properties of clean metals near quantum critical points. These include the discovery of a metamagnetic quantum critical point in $\text{Sr}_3\text{Ru}_2\text{O}_7$,¹ the appearance of superconductivity at the antiferromagnetic critical point in CePd_2Si_2 ,² presumably unconventional superconductivity on the ferromagnetic side of the critical point in UGe_2 ,³ the triplet superconductivity of Sr_2RuO_4 ,⁴ (the origin of superconductivity is unknown in this material, but it has been argued that it is close to ferromagnetic and antiferromagnetic critical points⁵) and the recently discovered superconductivity in ZrZn_2 .⁶ These discoveries suggest investigation of other clean metallic compounds with weak itinerant ferromagnetism that might be driven to the critical point, *e.g.* under moderate pressure. Common features of these metallic ferromagnets are: a low saturation moment at 0 K, low magnetic ordering temperature, high magnetic susceptibility at 0 K and negative magnetoresistance. The essential feature is that the physics are dominated down to quite low temperature (at the critical point down to 0 K) by quantum fluctuations associated with the critical point - these are manifest in the magnetic, transport and thermodynamic properties, *e.g.* as non-Fermi liquid scalings. Thus, in searching for such systems, we seek materials that are near the critical point with respect to some experimentally variable parameter (like pressure) and that are magnetically soft so that the critical region has a reasonable extent.

Early on, it was reported that Sc_3In is such a weak itinerant ferromagnet that may be near such a critical point.⁷ However, in Sc_3In under pressure, the magnetic moment is enhanced, so that the critical point cannot be reached at least with modest compression.^{8–10} Here we report density functional studies that support the view that Sc_3In is indeed near a quantum critical point, and show that, while the ferromagnetism is enhanced under pressure, it is suppressed by uniaxial strain, suggesting non-hydrostatic pressure as a practical way to reach the quantum critical point.

The calculations were done using the general potential linearized augmented planewave (LAPW) method,¹¹ as implemented in the WIEN2k code.¹² Relativistic effects were included at the scalar relativistic level. However, we verified that the magnetic moment at the

experimental structure is not sensitive to the inclusion of spin-orbit. This is presumably because the band structure near the Fermi energy is dominated by Sc *d* bands (see below). For the generalized gradient approximation (GGA) calculations, we used the exchange-correlation functional of Perdew, Burke and Ernzerhof.¹³ We chose the muffin-tin spheres $R_{MT} = 2.6$ a.u. and a basis set determined by a planewave cutoff of $R_{MT}K_{max} = 8.0$, which gives good convergence. The Brillouin zone samplings were done using the special \mathbf{k} points method with 528 points in the irreducible wedge of the hexagonal zone. Convergence was checked by varying the \mathbf{k} point density in the zone averages. Convergence was further checked by repeating some calculations with a different LAPW code^{14,15} using different sphere radii, local orbitals to relax linearization¹⁵ and a higher planewave cutoff, $R_{MT}K_{max} = 9.0$. This yielded essentially the same results.

Hexagonal Sc₃In occurs in the Ni₃Sn-type structure (spacegroup $P6_3/mmc$).¹⁶ The experimental lattice parameters are $a = 6.43$ Å and $c = 5.17$ Å.¹⁷ In this structure, the space group symmetry allows a free coordinate x , which has not been fixed experimentally and which gives the in-plane position of the Sc. However, it is expected based on solid state chemical reasoning (particularly the Sc coordination) that Sc should sit on the ideal site, $x=5/6$. We performed local density approximation and GGA calculations of the energy as a function of x to check this, and found that, to within the precision of our calculations, x indeed takes the ideal value of 5/6 in Sc₃In (the energy minimization yielded $x=0.832$); the calculated magnetic moment was found to be only weakly sensitive to changes in x of this order).

We show the paramagnetic electronic band structure calculated at the experimental crystal structure with the ideal value of x in Fig. 1, along with a blow-up of the region around E_F . The corresponding electronic density of states is given in Fig. 2. In the band structure, the Sc *d* character is indicated by the relative size of the plotting symbols. The two lowest valence bands lying between approximately -7 eV and -5 eV with respect to the Fermi energy, E_F , are In *s* derived, while the remaining valence bands beginning at -4 eV are formally described as Sc-In hybrids. However, from approximately -1 eV to several eV

above E_F , these are heavily dominated by Sc d states. The band structure near E_F shows two very flat Sc d derived bands as well as three more dispersive bands of mixed Sc d - In p character that pass through them. The flat bands lead to a prominent peak in the density of states (DOS) around E_F . The GGA DOS at E_F is $N(E_F) = 26.5 \text{ eV}^{-1}$ per unit cell (two formula units).

This peak underlies the itinerant ferromagnetism of Sc_3In , which occurs via the itinerant Stoner mechanism. We indeed find a ferromagnetic ground state in self-consistent calculations. The calculated GGA spin moment with the experimental structure is $3.0 \mu_B$ per unit cell (*i.e.* $0.50 \mu_B/\text{Sc}$). Again with the experimental crystal structure, local spin density approximation (LSDA) calculations give a smaller moment of $2.1 \mu_B$ also on a per unit cell basis ($0.35 \mu_B/\text{Sc}$). The magnetic energies, defined as the energy difference between constrained non-spin-polarized and ferromagnetic states, are very small – 1.3 mRy/Sc in the GGA and only 0.2 mRy/Sc in the LSDA. It is not unusual for GGA calculations to yield a somewhat greater tendency towards magnetism than the LSDA,¹⁸ but the magnitude of the difference here is large suggesting longitudinal magnetic softness. We note that both the LSDA and GGA spin magnetizations are considerably larger than experiment. Matthias *et al.* reported a magnetic moment of $0.051 \mu_B/\text{Sc}$, which is close to the value of $0.066 \mu_B/\text{Sc}$ found by Gardner *et al.* (Ref. 8). This level of disagreement may be taken as indicating the importance of quantum critical fluctuations in Sc_3In .

Density functional theory is in principle an exact ground state theory. It should, therefore, correctly describe the spin density of magnetic systems. However, common approximations to the exact density functional theory, such as the local spin density approximation (LSDA) and generalized gradient approximations (GGA), neglect Hubbard correlations beyond the mean field level, with the well known result that the magnetic tendency of strongly Hubbard correlated systems is often underestimated. Another type of correlations that are missed in these approximations are quantum spin fluctuations. This is because the LSDA and GGA are parameterized based on electron gasses with densities typical for atoms and solids. However, the uniform electron gas is very far from magnetism in this density

range. The result for non-collinear magnetism in molecules is well known - a so called “spin-contamination” in which the LSDA predicts classical magnetism, with *e.g.* non-quantized magnetic moments and singlets described with non-zero, static, but canceling, spin densities on various sites. In solids near quantum critical points, the result is an overestimate of the magnetic moments and tendency towards magnetism (*i.e.* misplacement of the position of the critical point) due to neglect of the quantum critical fluctuations. Since it is very uncommon for the LSDA to significantly overestimate the tendency towards magnetism away from such critical points, we take the overestimate found here as evidence for the importance of quantum critical fluctuations in Sc_3In . A similar overestimate was reported recently for ZrZn_2 ,¹⁹ which shows a critical point under pressure and coexistence of ferromagnetism and superconductivity.⁶ Similarly, in $\text{Sr}_3\text{Ru}_2\text{O}_7$, LSDA calculations predict a weakly ferromagnetic ground state,²⁰ while experimentally the material is a paramagnet very close to ferromagnetism.¹ Unfortunately, in Sc_3In , the ordinary method of reaching the critical point by applying hydrostatic pressure does not work, since, as mentioned, it is known that the magnetism of this compound becomes more robust under modest pressures.^{8–10}

In order to investigate this further and to see if there is another way of reaching the critical point, we performed GGA calculations of the total energy, magnetic moment and electronic structure as a function of the structural parameters c and a . These calculations were performed on a search grid with volume changes from -15% to +3% and c/a ratios from -40% to +40%, both with respect to the experimental structure. The internal parameter x was kept fixed at its ideal value during these calculations. A contour representation of the energy surface is given in Fig. 3. The calculated GGA structural parameters are in very close agreement with experiment. These were obtained by fitting the total energy surface $E(c/a, V)$ to a polynomial. The resulting equilibrium volume is $V = 187 \text{ \AA}^3$ per unit cell with the calculated $c/a = 0.809$. The experimental values are $V = 185 \text{ \AA}^3$ and $c/a = 0.804$.⁹ The calculated GGA constrained bulk modulus is 64 GPa (this is not strictly the same as the experimental bulk modulus as it is from a fit with a fixed c/a ratio, while experimentally c/a changes under hydrostatic pressure).

The variation of the calculated GGA spin moment as a function of V and c/a is shown in Fig. 4. The magnetic moment increases weakly under modest compression in agreement with the experimental trend,⁸ and then decreases, but only weakly, at high compressions. Volume compressions above 16% are needed before the GGA spin magnetization falls below its zero pressure value. The variation with c/a is stronger and more interesting. In particular, we find that the GGA magnetization has a maximum very close to the experimental c/a , which is also the c/a ratio for which E_F is in the center of the two heavy bands giving rise to the DOS peak that underlies magnetism. As c/a is changed these bands shift with respect to E_F and so as expected from extended Stoner theory the spin moment and magnetic energy is reduced.²¹

Considering the importance of quantum critical fluctuations, which strongly reduce the GGA magnetization, we cannot predict the position of the critical point. However, it is clear that Sc_3In is close to the critical point and that the magnetism can be suppressed with variations in the c/a ratio. Accordingly, we expect that the critical point can be reached under modest uniaxial strain. Experimental investigation of the low temperature magnetic, thermodynamic and transport properties of high quality single crystals of Sc_3In under uniaxial strain should be quite interesting.

We are grateful for helpful conversations with A.J. Millis, D. Mandrus I.I. Mazin and B.C. Sales. Work at the Naval Research Laboratory is supported by the Office of the Naval Research.

REFERENCES

¹ S.A. Grigera, R.S. Perry, A.J. Schofield, M. Chiao, S.R. Julian, G.G. Lonzarich, S.I. Ikeda, Y. Maeno, A.J. Millis, and A.P. Mackenzie, *Science* **294**, 329 (2001).

² N.D. Mathur, F.M. Grosche, S.R. Julian, I.R. Walker, D.M. Freye, R.K.W. Haselwimmer, and G.G. Lonzarich, *Nature* **394**, 39 (1998).

³ S.S. Saxena, P. Agarwal, K. Ahilan, F.M. Grosche, R.K.W. Haselwimmer, M.J. Steiner, E. Pugh, I.R. Walker, S.R. Julian, P. Monthoux, G.G. Lonzarich, A. Huxley, I. Sheikin, D. Braithwaite, and J. Flouquet, *Nature* **406**, 587 (2000).

⁴ Y. Maeno, H. Hashimoto, K. Yoshida, S. Nishizaki, T. Fujita, and J.G. Bednorz, and F. Lichtenberg, *Nature* **372**, 532 (1994).

⁵ I.I. Mazin and D.J. Singh, *Phys. Rev. Lett.* **82**, 4324 (1999).

⁶ C. Pfleiderer, M. Uhlärz, S.M. Hayden, R. Vollmer, H. von Lohneysen, N.R. Bernhoeft, and G.G. Lonzarich, *Nature* **412**, 58 (2001).

⁷ B.T. Matthias, A.M. Clogston, H.J. Williams, E. Corenzwit, and R.C. Sherwood, *Phys. Rev. Lett.* **7**, 7 (1961).

⁸ W.E. Gardner, T.F. Smith, B.H. Howlett, C.W. Chu, and A. Sreedler, *Phys. Rev.* **166**, 577 (1968).

⁹ J. Grewe, J.S. Schilling, K. Ikeda, K.A. Gschneidner, Jr., *Phys. Rev. B* **40**, 9017 (1989).

¹⁰ P.C. Riedi, J.G. Armitage, and R.G. Graham, *J. Appl. Phys.* **69** 5680 (1991).

¹¹ D.J. Singh, *Planewaves, Pseudopotentials and the LAPW Method* (Kluwer Academic, Boston, 1994).

¹² P. Blaha, K. Schwarz, G. K. H. Madsen, D. Kvasnicka and J. Luitz, WIEN2k, An Augmented Plane Wave + Local Orbitals Program for Calculating Crystal Properties (K. Schwarz, Techn. Universitt Wien, Austria), 2001. ISBN 3-9501031-1-2

¹³ J.P. Perdew, K. Burke and M. Ernzerhof, Phys. Rev. Lett. **77**, 3865 (1996).

¹⁴ S.H. Wei and H. Krakauer, Phys. Rev. Lett. **55**, 1200 (1985).

¹⁵ D. Singh, Phys. Rev. B **43**, 6388 (1991).

¹⁶ A. Palenzona, P. Manfrinetti, and R. Palenzona, J. Alloys and Compounds **243**, 182 (1996).

¹⁷ S.P. Yatsenko, A.A. Semyannikov, H.O. Shakarov and E.G. Fedorova, J. Less. Comm. Met. **90**, 95 (1983).

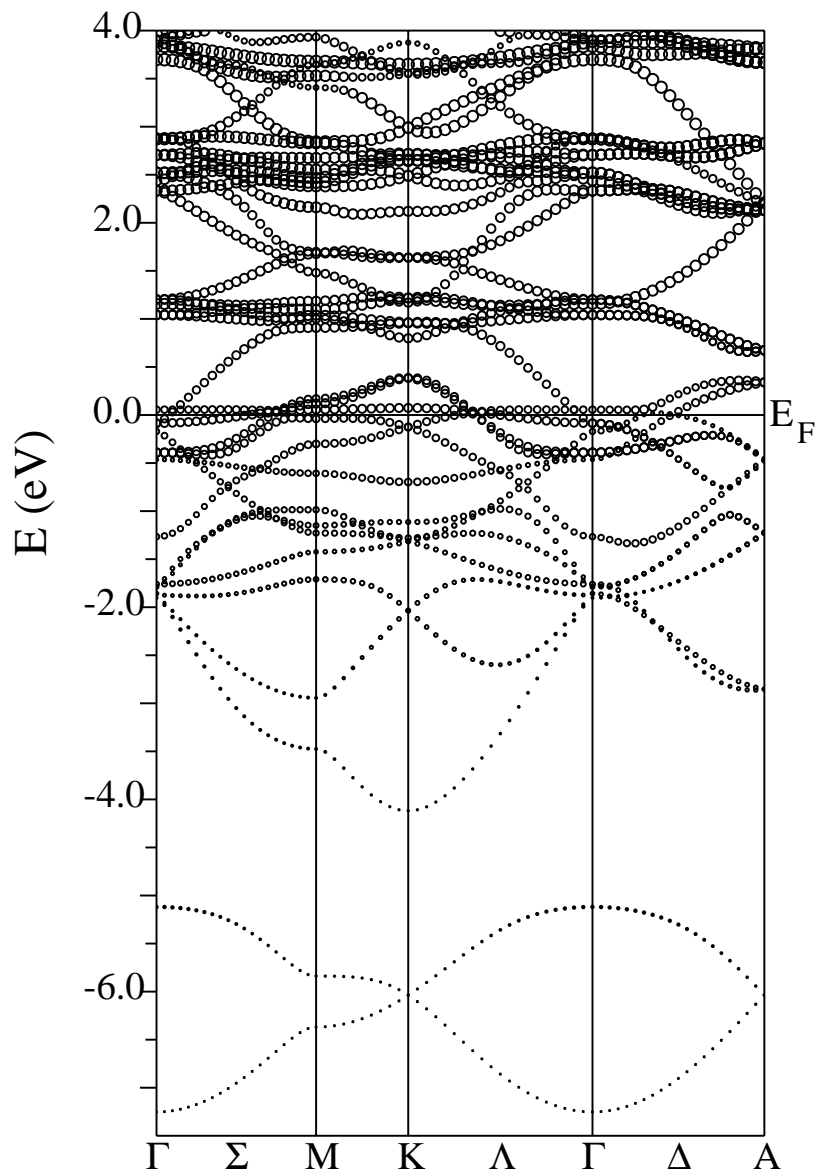
¹⁸ D.J. Singh and J. Ashkenazi, Phys. Rev. B **46**, 11570 (1992).

¹⁹ D.J. Singh and I.I. Mazin, Phys. Rev. Lett. **88**, 187004 (2002).

²⁰ D.J. Singh and I.I. Mazin, Phys. Rev. B **63**, 165101 (2001).

²¹ G.L. Krasko, Phys. Rev. B **36**, 8565 (1987).

FIGURES



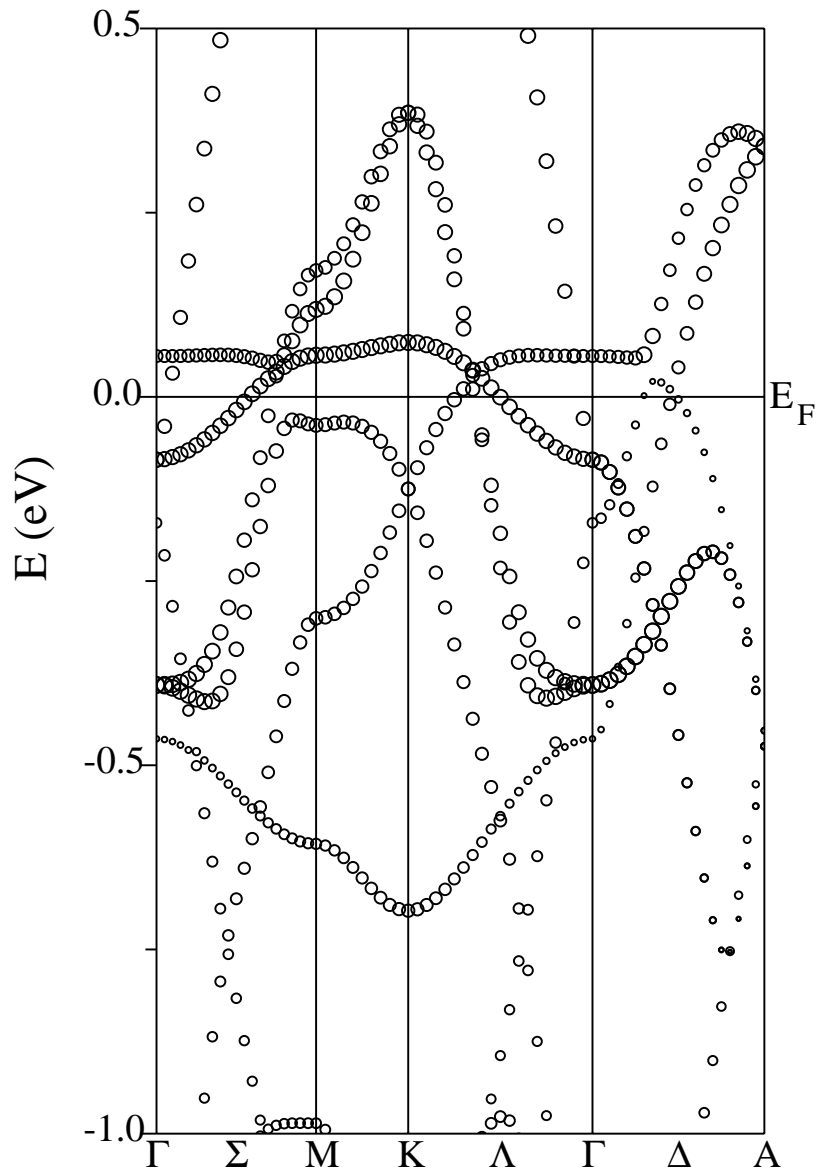


FIG. 1. Valence band structure of Sc_3In (top) and a blow-up around E_F (bottom). The radius of the plotting circles is proportional to $\text{Sc } d$ projection of the band.

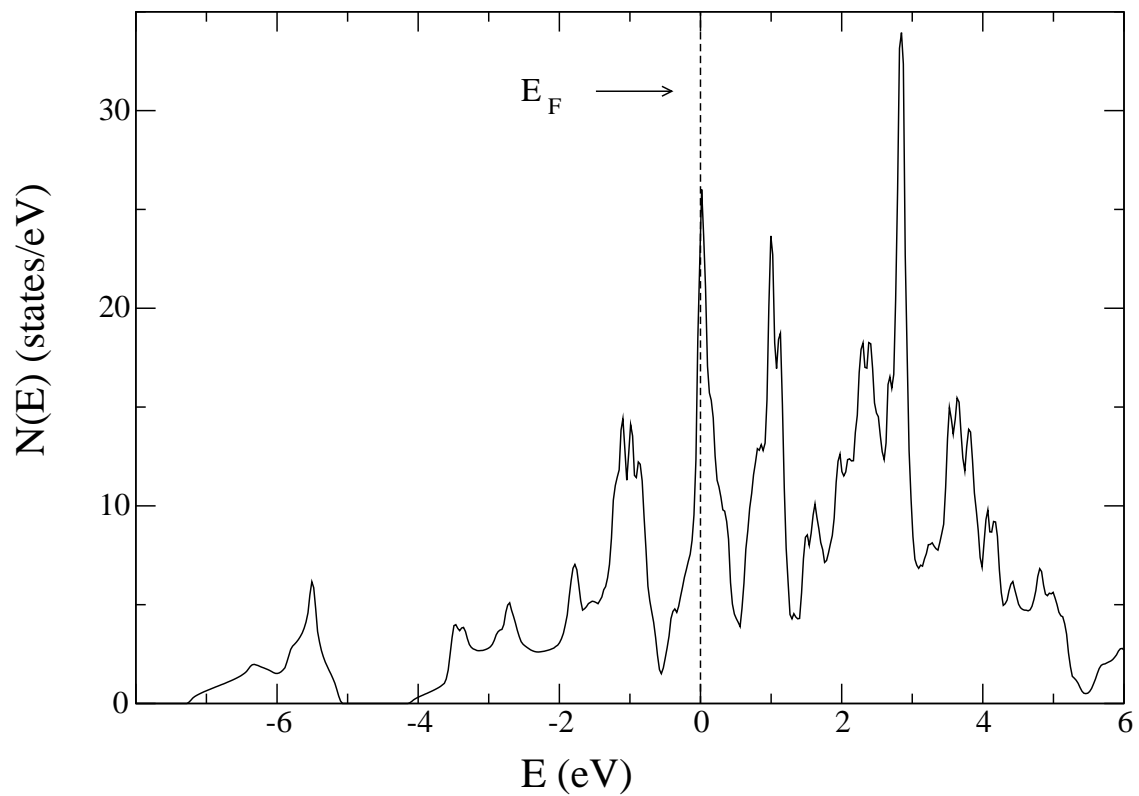


FIG. 2. Calculated electronic DOS on a per unit cell basis of non-spin-polarized Sc_3In obtained within the GGA. The zero is at E_F .

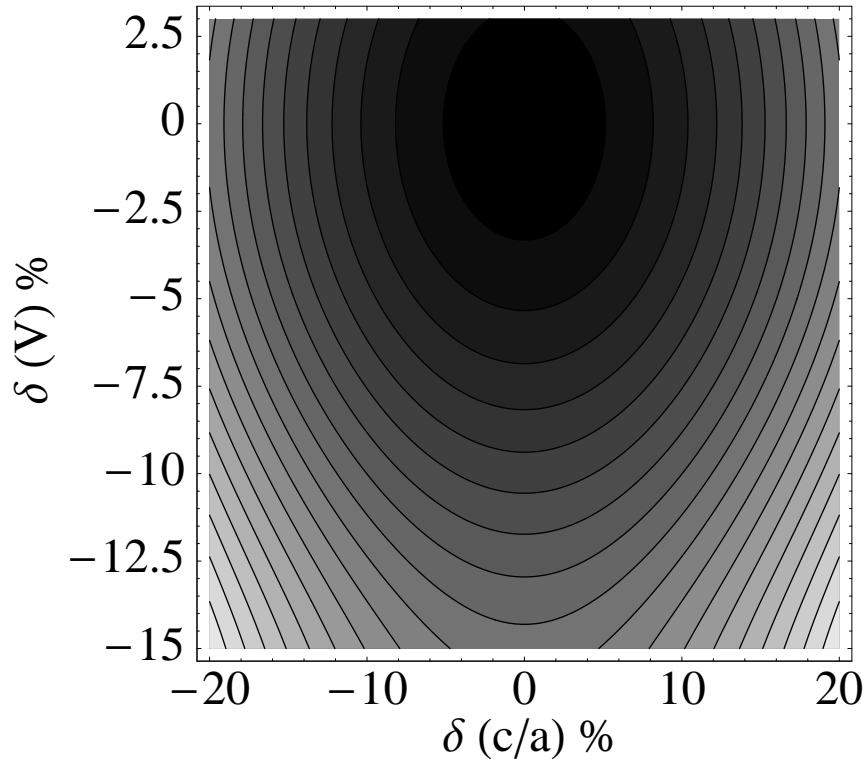


FIG. 3. Total energy surface as function of c/a and volume. $\delta(V)$ and $\delta(c/a)$ are the percentage deviations of V and c/a from their experimental values. The contours are spaced by 10 mRy per unit cell.

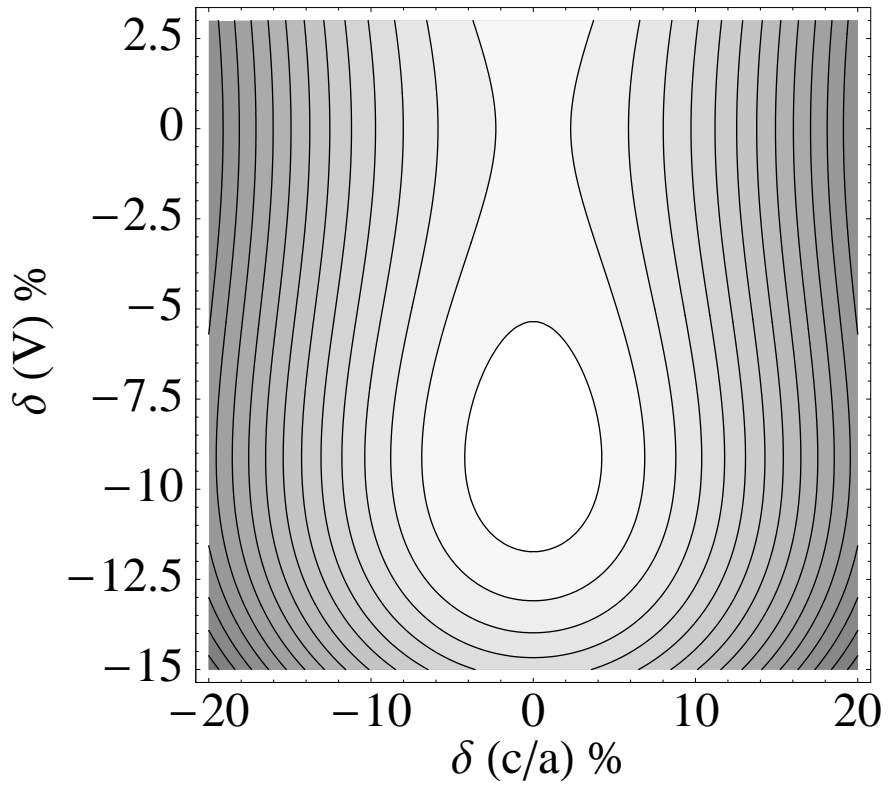


FIG. 4. Variation of the magnetic moment with c/a and volume as in Fig. 3. The contours are spaced by $0.10 \mu_B$ per unit cell.